High Energy Physics and Nuclear Physics

Volume 17, Number 2

Study of Antihydrogen-Atom Formation in Antiproton-Positronium Collisions

Cheng Zitao, Qian Qing, Fu Yunchang and Chen Xuejun

(Department of Physics, Tsinghua University, Beijing, China)

Some properties of antihydrogen-atom formations in antiproton-positronium collisions have been studied theoretically. The possibility of producing antihydrogen atoms in the laboratory is also discussed.

1. INTRODUCTION

A very interesting problem in experimental particle physics is the production of antihydrogen atoms in the laboratory. This is a long-standing and still unrealized dream [1]. According to theory, antihydrogen is predicted to be very stable in vacuum. If the antihydrogen atom could be formed in the laboratory, some fundamental research works would be possible, such as a test of the famous CPT invariance. The antihydrogen atom is one of the simplest and most fundamental systems in the antimatter world, just as the hydrogen atom in the matter world. Studies of its properties will improve our knowledge about the antimatter world; and studies of its interactions with hydrogen atoms, etc., will broaden our understanding on interactions of the antimatter world with the matter world. These are the main reasons for the continuing strong interest in the formation of antihydrogen atoms. Recently, this interest has been intensified due to the availability of an antiproton beam at the Low-Energy Antiproton Ring (LEAR) facility at CERN. Some people are preparing for such an experiment. Accordingly, it is reasonable to take a more serious theoretical study now.

The earliest idea for the antihydrogen atom formation is the radiative capture in positron-antiproton collisions,

---

Received on November 22, 1991. Supported by the Foundation of Graduate School and the Science School of Tsinghus University, China.

$$e^{+} + P \longrightarrow \bar{H} + \hbar\omega \tag{1}$$

However, in 1987 Humberston et al. [2] proposed another way to produce antihydrogen atoms in antiproton-positronium collisions,

$$\bar{P} + Ps \longrightarrow \bar{H} + e^{-} \tag{2}$$

According to the results of Humberston et al., the cross section for process (2) is about five times greater than that of process (1). Therefore, process (2) may be more valuable. In the present paper, we focus our attention on process (2). Obviously, in order to comprehend the characteristics of this process in detail it is necessary to calculate the integrated and differential cross sections.

Process (2) is a kind of rearrangement reactions, similar to the charge-exchange reaction. The first-order Born approximation is usually not enough to describe this kind of reaction, and higher order terms are needed [3]. Therefore, the result of the first order Born approximation can be regarded only as a qualitative reference, especially at low incident energies.

In the present paper, we adopt the multiple scattering expansion method proposed by one of the authors [4]. It has been proved that the first order approximation of this method is nearly equal to the sum of the first three orders in the Born expansion. Thus, the result deduced is highly reliable.

2. THEORY

The Hamiltonian H describing process (2) is

$$H = -\frac{1}{2}\nabla_1^2 - \frac{1}{2}\nabla_2^2 + \frac{1}{r_2} - \frac{1}{r_1} - \frac{1}{r} \tag{3}$$

Atomic units are adopted throughout this paper unless otherwise specified. In Eq.(3), r_1 and r_2 are the relative position vectors of the positron and electron with respect to the antiproton, respectively. Their relationship is shown in Fig.1. In writing Eq.(3), the antiproton is treated as a very heavy particle.

The total Hamiltonian can be decomposed in two ways:

$$H = H_i + V_i \quad \text{(entrance channel)} \tag{4}$$

where

$$H_i = -\frac{1}{2M}\nabla_R^2 - \frac{1}{2\mu}\nabla_r^2 - \frac{1}{r} \tag{5}$$

$$V_i = \frac{1}{r_2} - \frac{1}{r_1} \tag{6}$$

$$M = 2; \qquad \mu = \frac{1}{2} \tag{7}$$

or

$$H = H_f + V_f \quad \text{(exit channel)} \tag{8}$$

where

$$H_f = -\frac{1}{2}\nabla_1^2 - \frac{1}{r_1} - \frac{1}{2}\nabla_2^2 \tag{9}$$

$$V_f = \frac{1}{r_2} - \frac{1}{r} \tag{10}$$

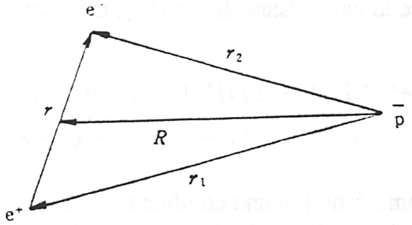

Fig. 1
The coordinate relationship $R = 1/2(r_1 + r_2)$, $r = r_1 + r_2$.

According to the general quantum collision theory [5], the differential cross section of reaction (2) can be written,

$$\frac{d\sigma}{d\Omega} = \frac{1}{2\pi^2}\frac{q_f}{q_i}|T|^2 \tag{11}$$

where, q_i and q_f are the incident and outgoing momenta, respectively, and T is the transition matrix element:

$$T = \langle \Psi_f^{(-)} | V_i | \Phi_i \rangle \tag{12}$$

$$= \langle \Phi_f | V_f | \Psi_i^{(+)} \rangle \tag{13}$$

Φ_i and Φ_f are the initial and final wave functions of the system, respectively; $\Psi_f^{(-)}$ is a complete wave function of the system corresponding to Φ_f, i.e., one of the eigenstates of H, satisfying the incident wave boundary condition; $\Psi_i^{(+)}$ has the same meaning.

How to derive $\Psi_i^{(+)}$ or $\Psi_f^{(-)}$ approximately is the main difference among the different theories. In this paper, the following two different methods are used:

a. Born expansion method

$\Psi_i^{(+)}$ is expressed as

$$\Psi_i^{(+)} = [1 + G_0V_i + G_0V_iG_0V_i + \cdots]\Phi_i \tag{14}$$

where G_0 is the free Green function. Thus, T can be written as:

$$T = T_B^{(1)} + T_B^{(2)} + T_B^{(3)} + \cdots \tag{15}$$

where

$$T_B^{(1)} = \langle \Phi_f | V_i | \Phi_i \rangle \quad \text{(1st order Born approximation)} \tag{16}$$

$$T_B^{(2)} = \langle \Phi_f | V_iG_0V_i | \Phi_i \rangle \quad \text{(2nd order Born approximation)} \tag{17}$$

$$T_B^{(3)} = \langle \Phi_f | V_iG_0V_iG_0V_i | \Phi_i \rangle \quad \text{(3rd order Born approximation)} \tag{18}$$

b. Multiple scattering expansion method [4]

$\Psi_f^{(-)}$ is written as,

$$\Psi_f^{(-)} = \Psi_M^{(1)} + \Psi_M^{(2)} + \cdots \tag{19}$$

In [4], the general multiple scattering expansion method is described in detail. The situation here is only a very simple and special case. According to [4], the forms of $\Psi_M^{(1)}$ and $\Psi_M^{(2)}$ etc. can be derived:

$$\begin{aligned}\Psi_M^{(1)} = \{&e^{iq_f\cdot r_2}\Gamma(1-i\eta)\Gamma(1+i\eta)F(i\eta,1,-i[q_f r_2+\boldsymbol{q}_f\cdot\boldsymbol{r}_2])\\ &F(-i\eta,1,-i[q_f r+\boldsymbol{q}_f\cdot\boldsymbol{r}])\}\phi_f(\boldsymbol{r}_1)\end{aligned} \tag{20}$$

where Γ and F are the gamma function and confluent super-geometric function, respectively. $\phi_f(\boldsymbol{r}_1)$ is the internal state wave function of the antihydrogen atom formed during the reaction. η is the Coulomb parameter, $\eta = 1/q_f$. The physical meaning of Eq.(20) is quite clear. The terms in the brackets stand for the distorted wave of the outgoing electron suffered from the antihydrogen nucleus and the positron outside the nucleus during the reaction. When the energy is very high, $\eta \to 0$, the distorted wave tends to a plane wave. Obviously, Eq.(20) possesses this quality.

The specific form of $\Psi_M^{(2)}$ is omitted here, because it is proved in [4] that, $\Psi_M^{(1)}$ is enough to provide a quite accurate result, i.e., nearly equal to the sum of the first three Born terms. Thus, according to the multiple scattering expansion method, T can be written as

$$T = T_M^{(1)} + T_M^{(2)} + \cdots \tag{21}$$

where

$$T_M^{(1)} = \langle\Psi_M^{(1)}|V_i|\Phi_i\rangle \tag{22}$$

$$T_M^{(2)} = \langle\Psi_M^{(2)}|V_i|\Phi_i\rangle \tag{23}$$

c. 1s-1s transition

In the following we first consider the main process, where, both of the P_s and the $\overline{\mathrm{H}}$ are in the 1s state. For such a process, ϕ_i and ϕ_f can be written as,

$$\phi_f(\boldsymbol{r}_1) = \frac{1}{\sqrt{\pi}}e^{-r_1} \tag{24}$$

$$\Phi_i = e^{i\boldsymbol{q}_i\boldsymbol{R}}\phi_i(\boldsymbol{r}) \tag{25}$$

and the 1s state wave function of P_s, ϕ_i is

$$\phi_i(\boldsymbol{r}) = \frac{1}{2\sqrt{2\pi}}e^{-r/2} \tag{26}$$

Thus $T_M^{(1)}$ can be specified as,

$$T_M^{(1)} = \frac{\eta}{2\sqrt{2}\,\mathrm{sh}(\pi\eta)}[A_M^{(1)} - B_M^{(1)}] \tag{27}$$

where

$$\begin{aligned}A_M^{(1)} = &\int d\boldsymbol{r}_2 d\boldsymbol{r}_1 e^{i\boldsymbol{q}_i\cdot\boldsymbol{R}}e^{-i\boldsymbol{q}_f\cdot\boldsymbol{r}_2}e^{-r_1}\frac{1}{r_2}e^{-\frac{r}{2}}\\ &F(-i\eta,1,i[q_f r_2+\boldsymbol{q}_f\cdot\boldsymbol{r}_2])F(i\eta,1,i[q_f r+\boldsymbol{q}_f\cdot\boldsymbol{r}])\end{aligned} \tag{28}$$

$$\begin{aligned}B_M^{(1)} = &\int d\boldsymbol{r}_2 d\boldsymbol{r}_1 e^{i\boldsymbol{q}_i\cdot\boldsymbol{R}}e^{-i\boldsymbol{q}_f\cdot\boldsymbol{r}_2}e^{-r_1}\frac{1}{r_1}e^{-\frac{r}{2}}\\ &F(-i\eta,1,i[q_f r_2+\boldsymbol{q}_f\cdot\boldsymbol{r}_2])F(i\eta,1,i[q_f r+\boldsymbol{q}_f\cdot\boldsymbol{r}])\end{aligned} \tag{29}$$

The calculations of $A_M^{(1)}$ and $B_M^{(1)}$ directly from Eqs.(28) and (29) are six-dimension integral problems. By using the method described in paper [6], Eqs.(28) and (29) can be reduced to an one-dimension and a two-dimension integrals, which makes the numerical calculations much easier. For this reason Eqs.(28) and (29) are changed into the following integrals:

$$A_M^{(1)} = \frac{\partial^2}{\partial\lambda_2\partial\lambda_3}\int d\boldsymbol{r}_2 d\boldsymbol{r}\, e^{-i\boldsymbol{p}_i\cdot\boldsymbol{r}_2}\frac{e^{-\lambda_1 r_2}}{r_2}F(-i\eta,1,i[q_f r_2 - \boldsymbol{q}_f\cdot\boldsymbol{r}_2]) \\ e^{-i\boldsymbol{p}_2\cdot\boldsymbol{r}}\frac{e^{-\lambda_2 r}}{r}F(i\eta,1,i[q_f r - \boldsymbol{q}_f\cdot\boldsymbol{r}])\frac{e^{-\lambda_3 r_1}}{r_1} \tag{30}$$

$$B_M^{(1)} = \frac{\partial^2}{\partial\lambda_1\partial\lambda_2}\int \mathrm{d}\boldsymbol{r}_2 \mathrm{d}\boldsymbol{r}\, e_{-i\boldsymbol{p}_i\cdot\boldsymbol{r}_2}\frac{e^{-\lambda_1 r_2}}{r_2}F(-i\eta,1,i[q_f r_2 - \boldsymbol{q}_f\cdot\boldsymbol{r}_2]) \\ e^{-i\boldsymbol{p}_2\cdot\boldsymbol{r}}\frac{e^{-\lambda_2 r}}{r}F(i\eta,1,i[q_f r - \boldsymbol{q}_f\cdot\boldsymbol{r}])\frac{e^{-\lambda_3 r_1}}{r_1} \tag{31}$$

Have

$$\boldsymbol{P}_1 = \boldsymbol{q}_i - \boldsymbol{q}_f; \qquad \boldsymbol{P}_2 = -\frac{1}{2}\boldsymbol{q}_i \tag{32}$$

λ_1, λ_2 and λ_3 are temporal parameters. After the computation the following value are taken

$$\lambda_1 = 0; \quad \lambda_2 = \frac{1}{2}; \quad \lambda_3 = 1 \tag{33}$$

According to the method in [6], $A_M^{(1)}$ and $B_M^{(1)}$ can be simplified

$$A_M^{(1)} = D_1(t=0) + \frac{\mathrm{sh}(\pi\eta)}{\pi i}\int_{-\infty}^{+\infty}\mathrm{d}y\,\frac{e^{(1+i\eta)\eta}}{1+e^{\eta}}[D_1(t) - D_1(t=0)] \tag{34}$$

$$B_M^{(1)} = D_2(t=0) + \frac{\mathrm{sh}(\pi\eta)}{\pi i}\int_{-\infty}^{+\infty}\mathrm{d}y\,\frac{e^{(1+i\eta)\eta}}{1+e^{\eta}}[D_2(t) - D_2(t=0)] \tag{35}$$

where

$$t = \frac{1}{1+e^{y}} \tag{36}$$

$$D_1(t) = 16\pi^2\int_0^{\infty}\mathrm{d}s\,\frac{\partial^2}{\partial\lambda_2\partial\lambda_3}\left[\frac{1}{\sigma_0}\left(\frac{\sigma_0}{\sigma_0+\sigma_1}\right)^{i\eta}\right] \tag{37}$$

$$D_2(t) = 16\pi^2\int_0^{\infty}\mathrm{d}s\,\frac{\partial^2}{\partial\lambda_1\partial\lambda_2}\left[\frac{1}{\sigma_0}\left(\frac{\sigma_0}{\sigma_0+\sigma_1}\right)^{i\eta}\right] \tag{38}$$

$$\sigma_0 = \{(\boldsymbol{p}_1+\boldsymbol{p}_2)^2 + (\lambda_1+\lambda_2)^2 + 2[(\boldsymbol{p}_1+\boldsymbol{p}_2)\cdot\boldsymbol{q}_f - i(\lambda_1+\lambda_2)q_f]t\} \\ (s^2+2\lambda_3 s) + 2s[\tilde{\lambda}_1(\lambda_3^2+\lambda_2^2+P_2^2) + \lambda_2(\lambda_3^2+\tilde{\lambda}_1^2+Q_1^2)] \\ + [(\tilde{\lambda}_1+\lambda_3)^2 + Q_1^{\,2}][(\lambda_2+\lambda_3)^2 + P_2^2] \tag{39}$$

$$\sigma_1 = 2[(\boldsymbol{p}_1+\boldsymbol{p}_2)\cdot\boldsymbol{q}_f - iq_f(\lambda_1+\lambda_2)](s^2+2\lambda_3 s) \\ + 2s[2\tilde{\lambda}_1(\boldsymbol{p}_2\cdot\boldsymbol{q}_f - i\lambda_2 q_f) - iq_f(\lambda_3^2+Q_1^2+\tilde{\lambda}_1^2)] \\ + 2[(\tilde{\lambda}_1+\lambda_3)^2 + Q_1^2][\boldsymbol{p}_2\cdot\boldsymbol{q}_f - i(\lambda_2+\lambda_3)q_f] \tag{40}$$

Q and $\tilde{\lambda}_1$ are defined as:

$$Q_1 = p_1 + q_f t \tag{41}$$

$$\tilde{\lambda}_1 = \lambda_1 - i q_f t \tag{42}$$

Using the same method, the first-order Born approximation result can be obtained:

$$T_B^{(1)} = \frac{1}{2\sqrt{2}\pi} D_B(t=0) \tag{43}$$

where

$$D_B(t) = 16\pi^2 \int_0^\infty \mathrm{d}s \left(\frac{\partial^2}{\partial\lambda_2 \partial\lambda_3} - \frac{\partial^2}{\partial\lambda_1 \partial\lambda_2} \right) \left(\frac{1}{\sigma_0} \right) \tag{44}$$

3. RESULT AND DISCUSSION

Based on above formulas, the differential and integrated cross sections can be calculated numerically. Within the framework of the multiple scattering expansion, the calculation can be reduced to one-dimension and a two-dimension integral problems; in the first-order Born approximation, the calculation is just a one-dimension integral. Numerical integrals are carried out by using the double precision Gaussian integral method. The choice of the number of Gaussian points and the integral region are enough to ensure that the numerical error is less than 5%. As a typical example, the y integral region is [-10,50], the number of Gauss points is 160, the s integral region is [0,100] and the number of Gauss points is 320.

Figures 2-6 are part of the results. The incident antiproton energies are 1, 2.5, 5, 10, 100 keV, respectively. The horizontal coordinate is the outgoing angle of the antihydrogen atom after the

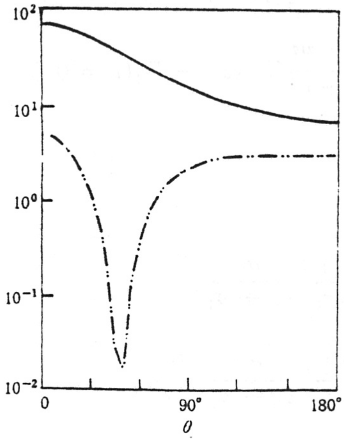

Fig. 2

The differential cross section of the antihydrogen atom formation (a_0^2/sr), at E_p = 1 keV.

The dashed curve is the result of the first-order Born approximation, and the solid curve is that of the first-order multiple scattering expansion approximation.

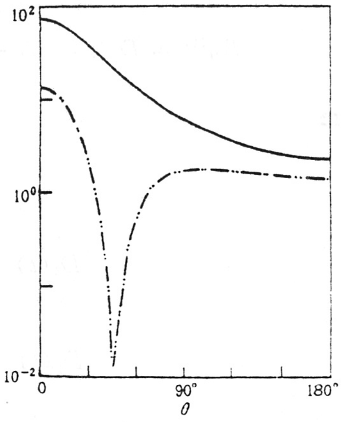

Fig. 3

Same as Fig.2, except that the energy of the antiproton is 2.5 keV.

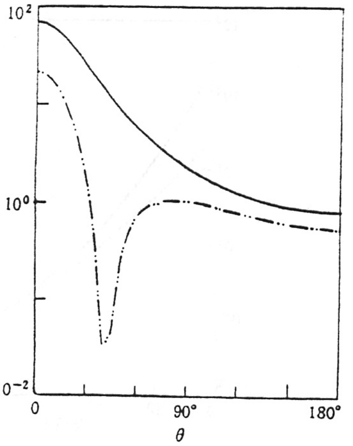

Fig. 4
Same as Fig.2, except that the energy of the antiproton is 5 keV.

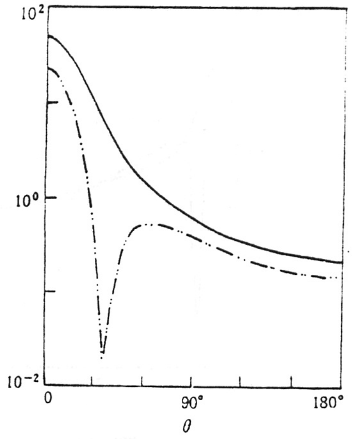

Fig. 5
Same as Fig.2, except that the energy of the antiproton is 10 keV.

reaction; the vertical coordinate is the differential cross section. The vertical axis is in atomic unit, i.e., $[a^2/\mathrm{sr}]$, where a_0 is the Bohr radius. The dashed curves stand for the results of the first order Born approximation, and the solid curves for that of the first order multiple scattering expansion approximation. Fig.7 shows the integrated cross sections as a function of the incident antiproton energies.

We conclude from our result:

1) The cross section of the $\overline{\mathrm{H}}$ formation through process (2) is much greater than the typical cross sections in particle and nuclear physics. Therefore, process (2) may be one of the desirable ways to produce antihydrogen atoms in the laboratory. The keypoint here is that there should be enough $\overline{\mathrm{p}}$ and P_s.

2) The integrated cross section of process (2) increases as the incident energy decreases (note that process (2) is an energy-releasing reaction), so it is favorable to use low energy $\overline{\mathrm{p}}$ beam. But as far as the angular distribution is concerned, with the energy decreasing the forward tendency of the angular distribution becomes weaker. This is not beneficial to the discrimination and full use of the $\overline{\mathrm{H}}$ atoms.

3) At low incident energies, the difference between the first order Born approximation and that of the first-order multiple scattering expansion approximation is fairly big; but with the energy increasing, e.g., 100 keV, the difference tends to vanish, except in the neighborhood of the deep valley.

4) All of the angular distributions in the first-order Born approximation have the valley feature. But this is not clear in the first multiples scattering expansion approximation. Which one is correct? Although this should be decided by future experiments at last, a judgement can be made now. Similar to the charge exchange reaction, e.t., $\mathrm{H}^+ + \mathrm{H}(1s) \rightarrow \mathrm{H}(nl) + \mathrm{H}^+$, process (2) belongs to the rearrangement reaction. In the first-order Born approximation, the angular distribution of the charge exchange reaction has the valley feature too. However, the valley does not exist in the result of a more accurate theory, especially not in the experiments. It follows that the valley phenomena do not exist in reality and its emergence is due to the defect of the Born approximation itself. The result of the multiple scattering expansion approximation may be closer to the real case.

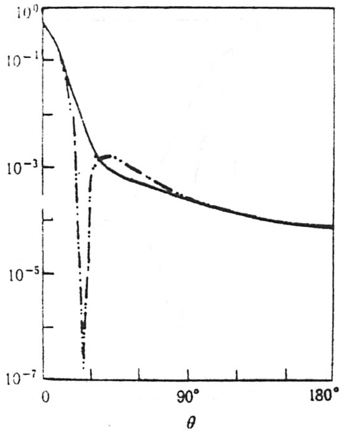

Fig. 6

Same as Fig.2, except that the energy of the antiproton is 100 keV.

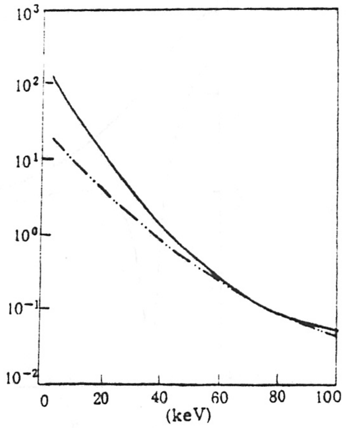

Fig. 7

The integral cross sections of the $\overline{H}$ formations (a_0^2) as a function of the incident energy of $\overline{p}$.

The dashed curve is the result of the first-order Born approximation, and the solid curve is that of the first-order multiple scattering expansion approximation.

5) The cross section in the first-order multiple scattering expansion approximation is much greater than that in the first-order Born approximation, especially for the low energy case. Naturally, this is favorable for the attempt to produce antihydrogen atoms in the laboratory.

6) Of course, to produce antihydrogen atoms in the laboratory is a hard and complicated job, which needs special studies. Besides P_s, is unstable and from the experimental viewpoint its lifetime is quite short. One can only use it while it is produced. It is a advisable method to produce P_s by electron-atom collisions. This question will be discussed in the next paper [6].

ACKNOWLEDGEMENT

The authors are grateful to Prof. Hu Jimin, Beijing University, for his support and help.

REFERENCES

[1] R. Neuman, H. Poth, A. Winnacker and A. Wolf, *Z. Phys.*, **A313**(1983)253.
[2] J.W. Humberston, M. Chalton, F.M. Jacobsen and B. Deutch, *J. Phys.*, **B20**(1987)L25.
[3] D. Belkic, R. Gayet and A. Salin, *Phys. Rep.*, **56**(1979)279.
[4] X.J. Chen, *Phys. Rev.*, **A40**(1989)1795.
[5] C.J. Joachain, Quantum Collision Theory (Amsterdam: North-Holland, 1975).
[6] Wen Bin et al., The Formation of Positronium, to be published in Transactions of Physics, China.